Available online at www.sciencedirect.com
SCIENCE DIRECT®
Pergamon
Cement and Concrete Research 34 (2004) 1321–1330
CEMENT AND CONCRETE RESEARCH

Influence of fracture process zone height on fracture energy of concrete

Xiaozhi Hu*, Kai Duan

School of Mechanical Engineering, University of Western Australia, Perth, WA 6009, Australia

Received 16 July 2003; accepted 16 December 2003

Abstract

The implication of modelling concrete fracture with a fictitious crack of zero fracture process zone (FPZ) height is addressed because FPZ height, in reality, is not zero and is bound to vary during crack growth. The ligament effect on fracture energy G_F is explained by the nonuniform distribution of a local fracture energy g_f showing the influence of specimen boundary and variation of FPZ height. The nonuniform g_f distribution is then used to determine the size-independent G_F. The recent boundary-effect model based on a bilinear g_f function is confirmed by the essential work of fracture (EWF) model for the yielding of deeply notched polymer and metal specimens. The EWF model provides a theoretical basis for the bilinear g_f distribution. The principal rationale of the boundary-effect model, the influence of FPZ height on fracture energy, is supported by experimental observations of thickness effect on fracture toughness of thin polymeric adhesives between metals.

Keywords: Fracture energy; Size effect; Boundary effect; Ligament effect; Fracture process zone

1. Introduction

Concrete, being a coarse-structured composite, has, for years, posed a challenge to those who have faith in fracture mechanics and who believe that its applications could bring more efficient usage of various types of concrete and provide an insight into the mystery of microstructure influence on concrete fracture. The non-LEFM problems facing the concrete community are not confined to concrete only. Similar problems do exist in many other material systems such as the common and well-known elastic and plastic fracture of metal and polymer, large-scale yielding of those ductile materials, and thickness effect on thin adhesive fracture. Those non-LEFM phenomena existing in very different material systems may appear unrelated at first glance, but a detailed assessment on the cause of those non-LEFM phenomena will reveal otherwise. Those non-LEFM phenomena are very similar in reality and are all induced by the interactions of the crack-tip fracture process zone (FPZ) with nearby material boundaries.

More than 10 years ago, one of the authors [1,2] made a postulation on concrete fracture and the associate ligament effect on the specific fracture energy G_F defined by RILEM [3]. It was speculated that the FPZ height h_{FPZ} was proportional to the fracture energy dissipation at the crack tip. If h_{FPZ} varied during crack growth, the crack-tip fracture energy dissipation would also vary, leading to a nonuniform fracture energy distribution along the crack path. This rationale was then used to introduce the concept of local fracture energy g_f. It was assumed that the local specific fracture energy g_f varied along a crack path following the variation of the FPZ height h_{FPZ}. Consequently, any single fracture energy measurement, such as the RILEM G_F, was only a rough indication of the nonuniform local fracture energy distribution along the crack path. The ligament or crack-length dependence of RILEM fracture energy was thus an indirect reflection on the existence of a nonuniform fracture energy dissipation in a concrete specimen. It had been shown that the g_f distribution along the crack path could be readily determined from the ligament-dependent RILEM fracture energy, and it was not necessary to directly measure variations of h_{FPZ} during crack growth for the determination of g_f.

Ten years have passed since the original proposal of local fracture energy g_f; the overall knowledge on concrete fracture has been greatly improved. Further progress [4–8]

* Corresponding author. Tel.: +61-8-938-02812; fax: +61-8-9380-1024.
E-mail address: xhu@mech.uwa.edu.au (X. Hu).

0008-8846/$ – see front matter © 2004 Elsevier Ltd. All rights reserved.
doi:10.1016/j.cemconres.2003.12.027

on the nonuniform distribution of local fracture energy g_f has been made, and more experimental data have been found to support the original local fracture energy g_f concept. More importantly, the concept has been adopted by others [9,10] in their work on concrete fracture. Similar with the authors' work [1,2,4–8], they have also concluded that the size-independent fracture energy G_F can be reliably determined from the nonconstant g_f distribution, and testing of large concrete specimens is thus unnecessary.

For a postulation like the local fracture energy g_f to survive and thrive, solid theoretical and experimental evidence on h_{FPZ} variation and its direct influence on fracture properties has to be found. In addition, there has to be a need, in practice, to transform a fortuitous guess into a useful and dependable tool. Therefore, the primary objective of the present paper is to further affirm the local fracture energy g_f concept and the associated h_{FPZ} influence on the specific fracture energy G_F using a well-accepted and separately developed fracture mechanics model together with explicit experimental evidence of different material systems. The usefulness and generality of the local fracture energy g_f concept in different material systems are subsequently addressed.

2. Comparison between concrete FPZ and fictitious crack

Cracking activities during concrete fracture are not limited to the main crack surface, even after the influence of specimen thickness is ignored. A sketch of a concrete crack with a large FPZ of comparable length and height is shown in Fig. 1, together with a fictitious crack of zero FPZ height [1,11]. The

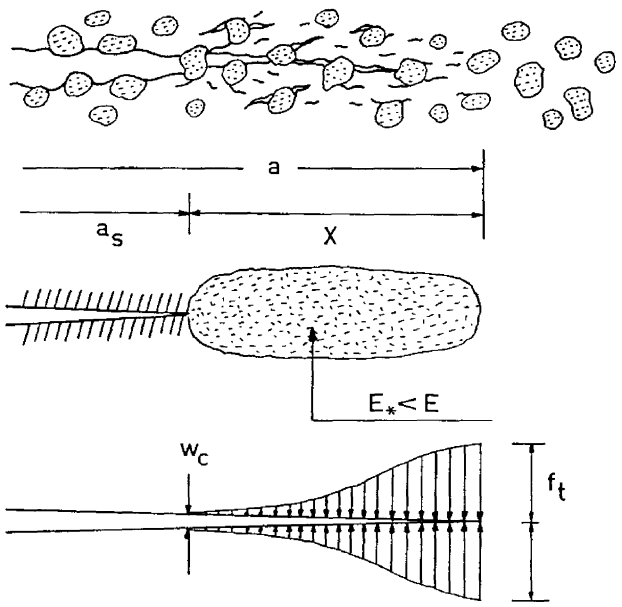

Fig. 1. Crack-tip FPZ in concrete, a damage zone model with $E^* < E$, and a fictitious crack model with distributed cohesive stresses, but zero FPZ height [1,11].

fictitious crack model [12,13], widely used to simulate concrete fracture, has simplified the real concrete FPZ of certain length and height by a bridged crack with cohesive stresses. The FPZ length is equal to the crack-bridging zone and, hence, its influence has been considered. However, the fictitious crack model has bypassed the FPZ height h_{FPZ} because of the simplified assumption that $h_{FPZ} = 0$.

The original explanation was that the FPZ height h_{FPZ} did not enter into the formulation of the fictitious crack model and, thus, the simplest and obvious assumption that $h_{FPZ} = 0$ was selected (e.g., Ref. [12]). The question why h_{FPZ} did not enter into the formulation of the fictitious crack model is far more important than the assumption of $h_{FPZ} = 0$. Mathematically, assuming that $h_{FPZ} = 0$ is the same as assuming $h_{FPZ} =$ constant. If h_{FPZ} indeed has any control over the concrete fracture process, its potential influence can only be indirectly reflected by the equivalent cohesive stress and crack opening relationship of a fictitious crack, which also defines the specific fracture energy G_F. Based on the same argument, any potential problems associated with the assumption $h_{FPZ} = 0$ will show up in the equivalent cohesive stress and crack opening relationship and the specific fracture energy G_F.

A valid transformation of a real concrete FPZ, with certain length and height into an equivalent fictitious crack with cohesive stresses over its surfaces but zero h_{FPZ}, is no doubt conditioned. The width of the damage zone ($E^* < E$) covering the total fracture area and the uneven main crack surface, as indicated in Fig. 1, is physically very different to a fictitious crack of zero h_{FPZ}. Therefore, the limitations and conditions of the fictitious crack model [12,13] with zero h_{FPZ} need to be well understood because they determine the degree of relevance of its prediction to real concrete fracture or to what extent practical applications of the model will be successful.

Interestingly, the very existence of cohesive stresses over a main crack surface in concrete requires a nonzero FPZ height. This is because the cohesive or crack bridging stresses in concrete have to come from a frictional pull out of aggregates and a tearing of various unbroken connections over the uneven main crack surface created by multiple cracking, which occurs in FPZ of certain length and height. Fig. 2 illustrates such a fracture process in concrete with a segmented FPZ [1,2] for simplicity and clarity. W_f specifies the width or height of the separated microcracking area that is related to the nonlinear stress and strain behaviour before the peak load. W_{sf} specifies the width or height of a strain-softening zone, which is then the FPZ height h_{FPZ}. As illustrated by the segmented zigzag crack surfaces, strain softening or cohesive stress would not exist if h_{FPZ} or W_{sf} were zero. Therefore, a nonzero critical crack opening displacement w_c, at which the cohesive stress drops to zero, has to be created by a nonzero W_{sf} or h_{FPZ}. It is known that the FPZ length or the cohesive stress zone is closely related to w_c. Therefore, both FPZ length and w_c cannot be separated, in reality, from a nonzero h_{FPZ}. The very existence of an FPZ of certain length has

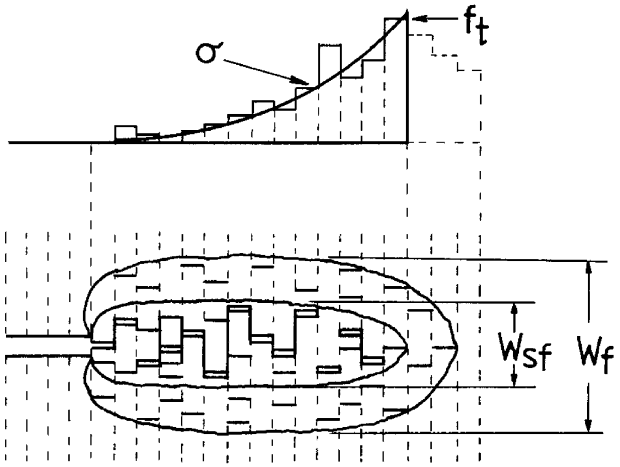

Fig. 2. Segmented FPZ and crack-bridging stress distribution. A nonzero FPZ height or inner softening zone width W_{sf} is required to generate crack bridging in concrete. The outer (micro-) fracture zone width W_f defines isolated cracking activities that are not related to softening or crack bridging [1,2].

virtually pronounced that $h_{FPZ}>0$. There would be no FPZ if h_{FPZ} were zero. In other words, the critical crack opening displacement w_c of a cohesive crack has to be zero if h_{FPZ} is zero. Since h_{FPZ} did not enter into the formulation of the fictitious crack model, the assumption of $h_{FPZ}=0$ was really the same as $h_{FPZ}=$ constant.

An FPZ can be fully developed in the centre of a relatively large concrete specimen that a fully developed h_{FPZ} can maintain its steady state at its maximum during crack growth. The delicate balance is upset and can no longer be maintained if the FPZ size is comparable to its distance to the closest specimen boundary. It can be envisaged that regardless how big a concrete specimen is, a crack tip will eventually approach the specimen back boundary in the final stage of crack growth. The crack-tip FPZ has to be reduced from its maximum size in length and height, which can only be acquired at the specimen centre due to the physical limitation of an unbroken ligament and the ever-changing stress gradient at the crack tip. Consequently, the degree of a zigzag crack path and associated strain softening is also changed. Fracture energy consumed in the creation of a steady-state FPZ, with the maximum h_{FPZ} in the centre of a specimen, simply cannot be the same with that consumed in the creation of a much reduced FPZ with a near-zero h_{FPZ}, close to a specimen boundary. It is thus not a surprise that the ligament effect has been commonly observed in the specific fracture energy of concrete because of the relatively large boundary region associated with its coarse material structure.

3. Comparison between global fracture energy G_f and local fracture energy g_f

The significance and usefulness of the specific fracture energy G_F defined by RILEM [3] in the analysis of cracked concrete structures are well recognised [9,10,12,13]. Experimental determination of G_F, following the RILEM definition, is yet remarkably simple. Only a stable load and load-point displacement ($P-\delta$) curve is required so that the total fracture energy $\int P\mathrm{d}\delta$ consumed in the process of breaking a notched concrete specimen into two pieces can be obtained from the stable $P-\delta$ curve. The RILEM G_F is defined as follows.

$$G_F=\frac{1}{B(W-a)}\int P\mathrm{d}\delta \tag{1}$$

where a is the initial notch or crack length, W is the specimen width in the crack growth direction, and B is the specimen thickness. It is clear from Eq. (1) that the RILEM G_F is simply the average of total fracture energy $\int P\mathrm{d}\delta$ over the total fracture area $B(W-a)$. It would be truly unconceivable that such a simple energy measurement, so roughly averaged over the entire fracture area, could remain constant and unaffected by the initial crack length and specimen size for whatever concrete specimens selected.

The size of a crack-tip FPZ in a normal concrete specimen can be quite large because of the coarse material structure of concrete, as illustrated in Fig. 1. No one expects the size of a crack-tip FPZ to remain constant during the entire fracture process, as FPZ is physically limited by the remaining uncracked ligament and is strongly influenced by the ever-changing stress gradient when a crack is approaching a specimen back boundary where $P\rightarrow 0$. While it is widely accepted that the fracture energy is dissipated within an FPZ of certain height and length during crack growth, it may not be so obvious to directly relate the variation of FPZ, particularly h_{FPZ}, to a nonuniform distribution of fracture energy dissipation along a crack path. However, it will be an obvious mistake to believe, without actually providing any physical evidence, that the fracture energy distribution over the entire crack path in a concrete specimen is always uniform.

Regardless how useful it is, G_F, as defined in Eq. (1), can only be taken as an average indication of the overall fracture energy dissipation because the total fracture energy $\int P\mathrm{d}\delta$ is averaged over the entire fracture area $B(W-a)$. The simple RILEM definition can also be explained in the following way without changing its physical meaning. The RILEM specific fracture energy G_F is a fracture energy distribution, which has been assumed to be uniform over the entire crack path; that is, a linear and constant distribution of the local fracture energy g_f exists so that $g_f=G_F=$ constant. If the RILEM definition is examined in this way, it is clear that the assumption is very rough and simply cannot be always correct, regardless whatever specimen size, geometry, and loading conditions are selected. Such a linear assumption has overlooked one important fact that FPZ, together with h_{FPZ}, changes from its maximum size when the crack tip is in the middle of a specimen to nearly zero when the crack

tip is close to the specimen back boundary, as discussed in the previous section.

If $g_f = G_F$ = constant, the specific fracture energy G_F can certainly be defined by the area under the crack-bridging stress and crack opening ($\sigma - w$) relationship, a fundamental material property used by the fictitious crack model [12,13] or the more general crack bridging models (e.g., Refs. [14–16]).

$$G_F = \int_0^{w_c} \sigma dw \tag{2}$$

where w_c is, again, the critical crack opening. The equivalence of Eqs. (1) and (2) has indeed been used to determine the σ–w relationship from experimental P–δ curves (e.g., Refs. [14,17,18]). When a constant w_c or single $\sigma - w$ relationship is applied to an entire $P - \delta$ curve, a constant h_{FPZ} has been virtually assumed for the entire crack path. The FPZ length variation during crack growth has no impact on G_F because G_F is the fracture energy dissipation per unit crack area, but h_{FPZ} is different. A $\sigma - w$ function determined from a complete $P - \delta$ curve should be treated with caution because h_{FPZ} is not constant in the boundary region where $P \to 0$. However, a good estimation on the steady $\sigma - w$ relationship can be obtained if only a part of the $P - \delta$ curve, with constant local fracture energy g_f, is used in numerical simulations, and the long tail of the $P - \delta$ curve after the peak load, for small P values, is ignored in curve fitting. In this case, the specific fracture energy $g_f = G_F$ = constant away from all boundaries is determined, and a single $\sigma - w$ relationship is determined from experimental $P - \delta$ curves as a material property.

As discussed above, the boundary region where h_{FPZ} is reduced should be avoided to determine the steady-state G_F. However, the "global" specific fracture energy G_F determined from a complete $P - \delta$ curve, as defined by Eq. (1), always includes the boundary region, which explains why the RILEM G_F is often ligament dependent. The influence of a varying h_{FPZ}, created by interactions of FPZ with the specimen back boundary, can become a dominant factor for G_F measurements if the initial uncracked ligament is short.

The local fracture energy g_f concept provides a simple and practical solution to the ligament effect on the global fracture energy by separating the boundary influence from the size independent G_F. If the ligament effect on the RILEM fracture energy exists, the specific fracture energy is initial notch dependent or crack-length dependent for a set of concrete specimens of identical size W. Let $G_f(a)$ be the crack-length- or ligament-dependent global specific fracture energy. The local fracture energy g_f concept shows that:

$$G_f(a) = \frac{1}{W-a}\int_0^{W-a} g_f dx = \frac{1}{W-a}\int P d\delta \tag{3}$$

where the position parameter x varies from zero at the initial crack tip to $W - a$ at the specimen back boundary. Eq. (3) shows that for a given initial notch or crack length a, a size-dependent global fracture energy $G_f(a)$ can be measured, following the RILEM definition, as given in Eq. (1). Testing concrete specimens of a fixed size W, but different crack-length a, produces not only the size-dependent global $G_f(a)$ measurements, but also the much-wanted information on the local g_f distribution.

One practical contribution of the local fracture energy g_f concept is that it also provides a simple way of finding the nonuniform g_f distribution using the crack-length-dependent $G_f(a)$ measurements [1,2].

$$g_f(a) = G_f(a) - (W-a)\frac{dG_f(a)}{da} \tag{4}$$

The crack-length- or ligament-dependent $G_f(a)$ is measured routinely using a complete $P - \delta$ curve, as specified by RILEM. The $G_f(a)$ variation with the initial notch or crack a can be easily determined by testing a set of concrete specimens of a fixed size W, but with different initial cracks. The $G_f(a)$ curve established for a range of a/W ratio (e.g., 0.2 to 0.9) can then be used to determine the local g_f distribution from Eq. (4). Given by Eq. (4), $g_f(a)$ shows the local specific fracture energy at location a (i.e., $x = 0$). A set of global $G_f(a)$ data is then transformed into a local $g_f(a)$ distribution over the tested a/W ratio range (e.g., 0.2 to 0.9) by Eq. (4). The typical trend of a global $G_f(a)$ curve of concrete observed in many experiments is illustrated schematically in Fig. 3a, together with the local $g_f(a)$ distribution that can be worked out from Eq. (4). The experimental $G_f(a)$ results of a mortar [1,2] are shown in Fig. 3b, which were used to determine the $g_f(a)$ curves shown in Fig. 3c.

The $G_f(a)$ results in Fig. 3b were analysed in two different ways. First, following the trend of experimental results, a Weibull function, the dashed line in Fig. 3b, was selected and applied to all experimental data. The specimen back boundary region was not predetermined, but it could be worked out from the resultant local $g_f(a)$ distribution using Eq. (4). Second, the specimen back boundary region was presumed to be in the range of $0.7 < a/W < 1$. A bilinear g_f function was then assumed in the following way: g_f = constant, away from the back boundary, and g_f was linearly reduced in the back boundary region for $a/W > 0.7$. The second assumption allowed the determination of the $G_f(a)$ function from Eq. (3), which was then used to fit the $G_f(a)$ results for $a/W < 0.7$, as the solid line in Fig. 3b. However, the two $g_f(a)$ distributions shown in Fig. 3c came out almost identical, indicating the boundary region where FPZ was altered because the physical limitation of the remaining ligament and sharp stress gradient was indeed around $a/W = 0.7$ for the specimen size and geometry. An almost identical linear g_f distribution in the boundary region for $a/W > 0.7$ had been obtained, although two different functions were used for curve fitting the $G_f(a)$ results in Fig. 3b, indicating that a linear function might be adequate to describe the local specific fracture energy g_f distribution in the boundary region due to the h_{FPZ} variation.

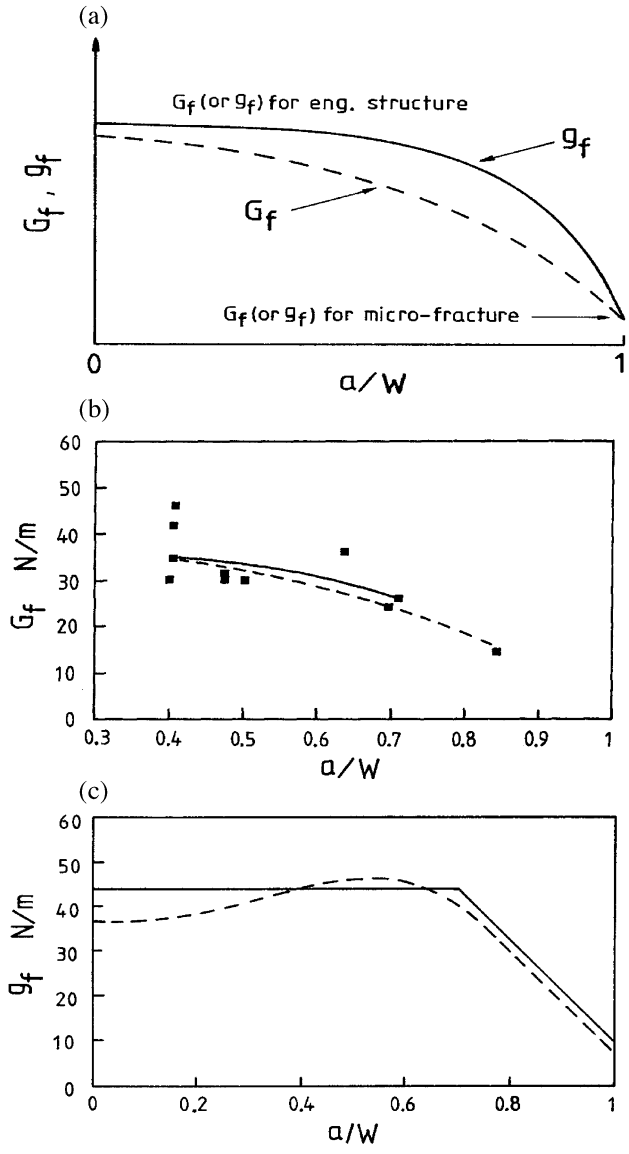

Fig. 3. (a) Initial-crack- or ligament-dependent RILEM G_f can be measured as function of a/W ratio; local fracture energy g_f distribution responsible for ligament effect on G_F is then determined [1,2]. (b) Experimental G_f results of a mortar. Curve fitting: solid line is based on the assumption of constant g_f for $a/W < 0.7$, and dash line is based on the assumption that G_f follows a Weibull distribution [1,2]. (c) The two local g_f distributions are determined from the two G_f curves in Panel b. The reduction of g_f in the boundary region, $a/W > 0.7$, is responsible for the ligament dependence of RILEM G_f [1,2].

It is important to know that the introduction of local specific fracture energy g_f does not require any new tests; the simple test for the global G_F shown in Eq. (1), as already adopted by RILEM, is what the local g_f requires. This has been clearly demonstrated by the results shown in Fig. 3. As shown in Fig. 3, the local specific fracture energy g_f concept provides an insight into the cause why the global $G_f(a)$ defined by RILEM is crack-length- or ligament-dependent and provides a simple method of analysing the size effect. The results in Fig. 3c imply that a simple bilinear function may be adequate enough to describe the g_f variations in the boundary region and the centre part of a specimen, away from all the boundaries. Such a bilinear g_f function can be taken as an extension of the assumption of a constant g_f distribution, i.e., $g_f = G_F = \text{constant}$ when Eq. (1) is used as defined by RILEM. If the specimen inner zone is dominant or the influence of a boundary region is small and can be neglected, the local specific fracture energy g_f is identical to the global specific fracture energy G_F as defined by RILEM. As a result, there is no size effect.

4. Bilinear simplification of local fracture energy

The local fracture energy g_f concept has recently been further simplified after the introduction of the clearly defined inner zone and boundary region described by a bilinear g_f distribution [4–8]. The bilinear g_f distribution over a specimen ligament $(W-a)$ and the variation of the FPZ size, particularly its height h_{FPZ}, are illustrated in Fig. 4. The RILEM-defined global specific fracture energy is shown as $G_f(a/W)$, as it depends on the initial crack a or initial a/W ratio. As can be seen from Fig. 4a, $G_f(a/W)$ is the average of the bilinear g_f distribution over the ligament $(W-a)$. In the inner zone, the size-independent material constant is found, where $G_F = g_f \equiv$ constant.

The explanation of the FPZ influence and the resultant bilinear g_f distribution illustrated in Fig. 4 is simple. In the inner zone, a crack-tip FPZ during crack growth can be fully developed, as it is away from the specimen back boundary, that the FPZ height h_{FPZ} remains constant at its maximum and $G_F = g_f \equiv$ constant. Only under such a condition, h_{FPZ} does not enter into the formulation of a fictitious crack, and hence can be assumed as zero. However, the inherent influence of h_{FPZ} on G_F has already been included in the equivalent cohesive stress and crack-opening relationship. In other words, a model fictitious crack with zero h_{FPZ} can be assumed only if the nonzero h_{FPZ} does not vary in reality. In this case, the RILEM G_F is size independent, and a unique $\sigma - w$ relationship, as shown in Eq. (2), exists.

In the boundary region, FPZ, and then its height h_{FPZ}, is inevitably reduced because of the physical limitation of the remaining ligament and ever-changing stress gradient. The variation in h_{FPZ} leads to the reduction in the local specific fracture energy g_f. The assumption of a fictitious crack with zero h_{FPZ} can still be used, but a unique $\sigma - w$ relationship does not exist. The local fracture energy g_f concept [1,2,8] has pointed out that the crack-bridging stress and crack-opening strain $(\sigma - w/w_c)$ relationship is more adequate. Such an assumption is similar with the nonlocal models [19,20] used to simulate concrete fracture with a large crack-tip FPZ, and they show the FPZ height h_{FPZ} indeed varies along the crack path.

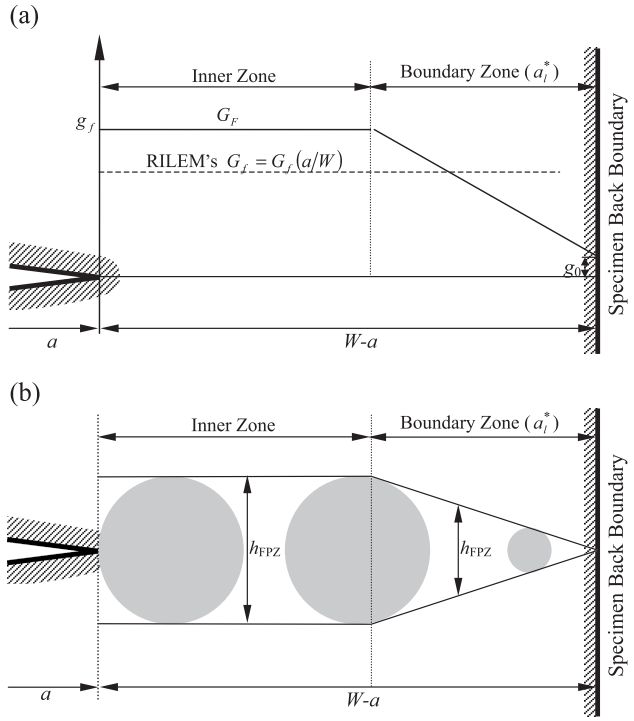

Fig. 4. (a) Separation of the inner zone and boundary region in a specimen of ligament $(W-a)$ and the bilinear g_f distribution. RILEM G_f is an average of the two linear g_f functions. (b) Corresponding variations of FPZ and its height in the inner zone and boundary region during crack growth.

Following the sketch in Fig. 4a, the local specific fracture energy g_f can be written as:

$$g_f = \begin{cases} G_F & W-a > a_l^* \quad \text{(a)} \\ g_0 + \frac{W-a}{a_l^*}(G_F - g_0) & W-a \le a_l^* \quad \text{(b)} \end{cases} \tag{5}$$

The size- or ligament-dependent global specific fracture energy G_f can then be determined from Eq. (3).

$$G_f = \begin{cases} G_F - \frac{a_l^*}{2(W-a)}(G_F - g_0) & W-a > a_l^* \quad \text{(a)} \\ g_0 + \frac{(W-a)}{2a_l^*}(G_F - g_0) & W-a \le a_l^* \quad \text{(b)} \end{cases} \tag{6}$$

The g_f and G_f relationship given in Eq. (4) can also be confirmed by the functions given in Eqs. (5) and (6). The bilinear assumption for g_f as shown in Eq. (5) gives the simple solutions for G_f shown in Eq. (6), which can then be used to fit the experimental data so that the size-independent G_F can be determined.

The usefulness of Eq. (4) is that it does not require any presumption for the local fracture energy g_f distribution. The curve fitting of experimental G_f results is done first, then, the obtained curve-fitting G_f function is used to work out the local fracture energy g_f distribution. In fact, the two different methods, assuming a bilinear g_f or curve-fitting G_f, have already been illustrated in the original local fracture energy g_f concept as shown in Fig. 3b and c.

If a concrete specimen has a short ligament $(W-a) < a_l^*$, only the boundary region exists, and Eq. (6b) indicates a linear relation between G_f and $W-a$. This will be the case if deeply notched specimens are used as shown in Fig. 3c for $a/W > 0.7$. In fact, deeply notched specimens have been frequently used to study large-scale yielding of polymers and metals. And indeed, the usefulness and significance of local fracture energy g_f concept can further be seen from the well-received essential work of fracture (EWF) model [21–24], proposed separately for deeply notched polymer and metal specimens.

5. Essential work of fracture

The EWF model was proposed to characterise fracture of deeply notched metal and polymer specimens through large-scale yielding [21–24]. Typical specimens tested to verify the EWF model are shown in Fig. 5, where the situations are identical with that of a concrete specimen with short ligament $(W-a) < a_l^*$. The fracture energy measurement, the specific work of fracture defined in the EWF model, is identical with the specific fracture energy defined by RILEM, as shown in Eq. (1), and is found to vary with the ligament length. For consistency, the global specific fracture energy G_f is used for the specific work of fracture used in the EWF model. The global G_f of concrete as given by Eq. (6b) is a linear function of $(W-a)$, with g_0 as its minimum value for microfracture, with near-zero h_{FPZ}.

The EWF model assumes that full ligament yielding precedes fracture for cases shown in Fig. 5. For simplicity, the yielding zone at the entire ligament has been approximated by a circular area, that the FPZ height h_{FPZ} is the same as the ligament length $(W-a)$. The global specific fracture energy G_f, as a total energy measurement, can be separated into the EWF (w_e) and the nonessential work of fracture or the plastic work (w_p). The specific fracture energy G_f is related to the ligament length $(W-a)$ or the FPZ height h_{FPZ} by

$$\begin{aligned} G_f &= w_e + w_p = w_e + \text{constant} \cdot (W-a) \\ &= w_e + \text{constant} \cdot h_{FPZ} \end{aligned} \tag{7}$$

That is, the EWF (w_e) is independent of the plastic zone size, and the plastic work (w_p) is given by the ratio of total plastic fracture energy over ligament area. The total plastic fracture energy is proportional to the total plastic zone volume, Length × Height × Thickness, or proportional to $(W-a)^2$ × Thickness. The ligament area is proportional to $W-a$ or Length × Thickness. Therefore, the ratio of total plastic fracture energy over the ligament area defines a linear relation between G_f and plastic zone height h_{FPZ} measured by $W-a$. It is clear that Eqs. (6b) and (7) are identical with $w_e = g_0$. The only difference is that Eq. (6) is not limited to deeply notched specimens, because Eq. (6a) covers situations where the inner zone may become dominant. However, Eq.

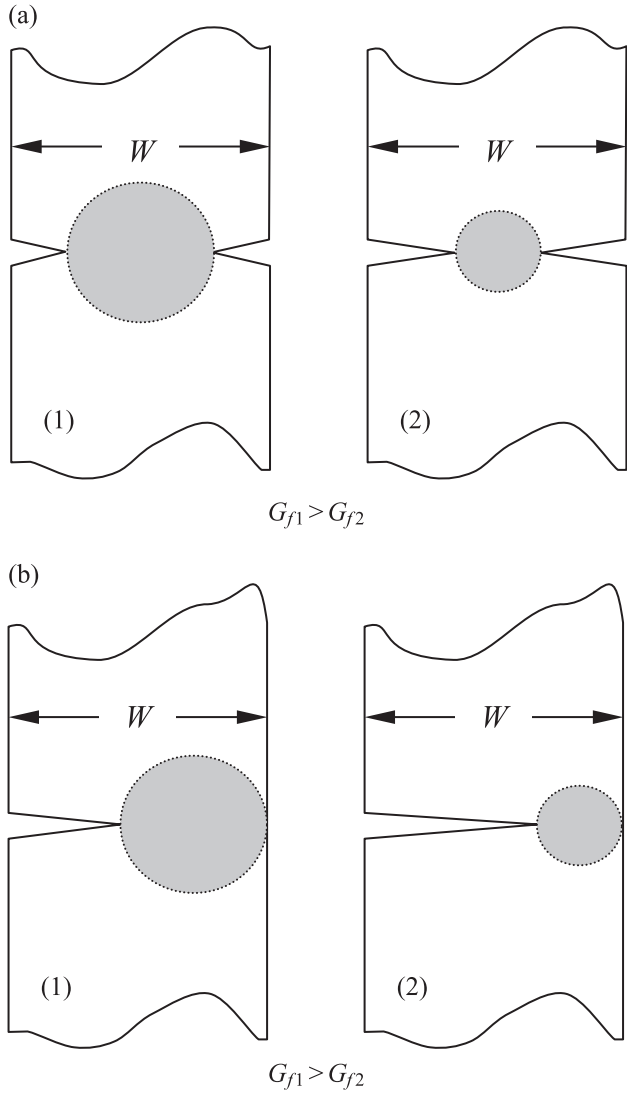

Fig. 5. (a) Full yielding in double-notched EWF specimens. (b) Full yielding in single-notched EWF specimens showing the influence of boundary region.

(7) provides a direct support to the assumed linear distribution of local specific fracture energy g_f in the boundary region, which leads to Eq. (6b).

The EWF w_e, together with G_f, has been measured for various metals and polymers [21–24] based on the linear relationship between G_f and $W-a$ or h_{FPZ}. The EWF model has been well proven in many experiments and is widely recognised. The EWF model defines a linear function of the local fracture energy g_f in the boundary region, and another linear function of g_f ($\equiv$ constant) is defined in the inner zone away from all boundaries. Therefore, the bilinear g_f function, considering local fracture energy distributions in the inner zone and boundary region, is the simplest alternative to otherwise the constant G_F assumption.

In comparison with the EWF w_e for polymer and metal, little work on g_0 has been done for concrete because a g_0 corresponding to zero h_{FPZ} is very small for concrete and is only a small fraction of the total fracture energy. This is evident from the g_f distributions shown in Fig. 3c. However, for the very reason, any g_f value higher than g_0 is highly h_{FPZ} dependent. That is why a bilinear g_f distribution needs to be adopted for small concrete specimens to consider the boundary influence, due to the variation in h_{FPZ}.

6. Thickness effect on fracture of adhesive joints

Yielding is confined within a thin adhesive used to bond two high-modulus substrates or two nonyielding boundary materials. The shape and size of a yielding zone or FPZ are strongly influenced by the boundaries, but the FPZ height h_{FPZ} is always equal to the adhesive thickness t for thin adhesives. This provides an ideal opportunity to characterise explicitly the influence of h_{FPZ} on the fracture properties of thin adhesives. It has been shown experimentally that the critical strain energy release rate G_C is proportional to h_{FPZ} or the adhesive thickness t for thin adhesives. The following model has been proposed by the authors [25] for adhesive fracture.

$$G_C = \begin{cases} g_0 + \frac{(G_{max}-g_0)}{t_{max}} t & t < t_{max} \text{ (a)} \\ G_{bulk} + (G_{max} - G_{bulk}) \left(\frac{t}{t_{max}}\right)^{-C\frac{G_{max}}{t_{max}}} & t > t_{max} \text{ (b)} \end{cases} \quad (8)$$

where C is an experimental constant, and G_{bulk} is the critical strain energy release rate measured with a bulk-adhesive specimen. At $t = t_{max}$, the maximum plastic zone or FPZ height is reached (maximum $h_{FPZ} \approx t_{max}$; [26,27]) so that $G_C = G_{max}$. Eq. (8b) shows how the boundary influence is diminishing with further increasing adhesive thickness t after $t > t_{max}$. Eq. (8a) for $t = h_{FPZ}$ is the same as Eqs. (6b) and (7); that is, the plastic zone or FPZ height h_{FPZ} controls the specific fracture energy and critical strain energy release rate.

Eq. (8), with $g_0 = 0$ and 0.5 kJ/m^2, is applied to the results with specimen thickness $B = 50$ mm in Fig. 6a [26], which gives $G_{max} = 4.41$ and 4.11 kJ/m^2, $t_{max} = 0.89$ mm, and $G_{bulk} = 1.40$ kJ/m^2. The constant C in Eq. (8b) for $t > t_{max}$ is 7.32 for G_{max} in kJ/m^2 and t_{max} in millimeters. The dimensionless number $C(G_{max}/t_{max})$ shows how fast G_C drops from G_{max} after $t > t_{max}$. It is noted that $G_{max} > G_{bulk}$ because the influence of the hard boundary material has induced a larger h_{FPZ} at t_{max}, which can never be achieved in the bulk adhesive without the boundary influence. The correlation between G_{max} and $h_{FPZ} = t_{max}$ has once again showed the importance of the FPZ or plastic zone height h_{FPZ}. If h_{FPZ} varies, G_C and G_f follow. If $h_{FPZ} = t_{max} >$ the stable FPZ height attainable in the bulk material, then, $G_{max} > G_{bulk}$.

Using the same constant C (7.32), t_{max} (0.89 mm), and g_0 (0 and 0.5 kJ/m^2), Eq. (8) is applied to the results with specimen thickness $B = 3$ mm. The predictions, together with the experimental data, are shown in Fig. 6b, where

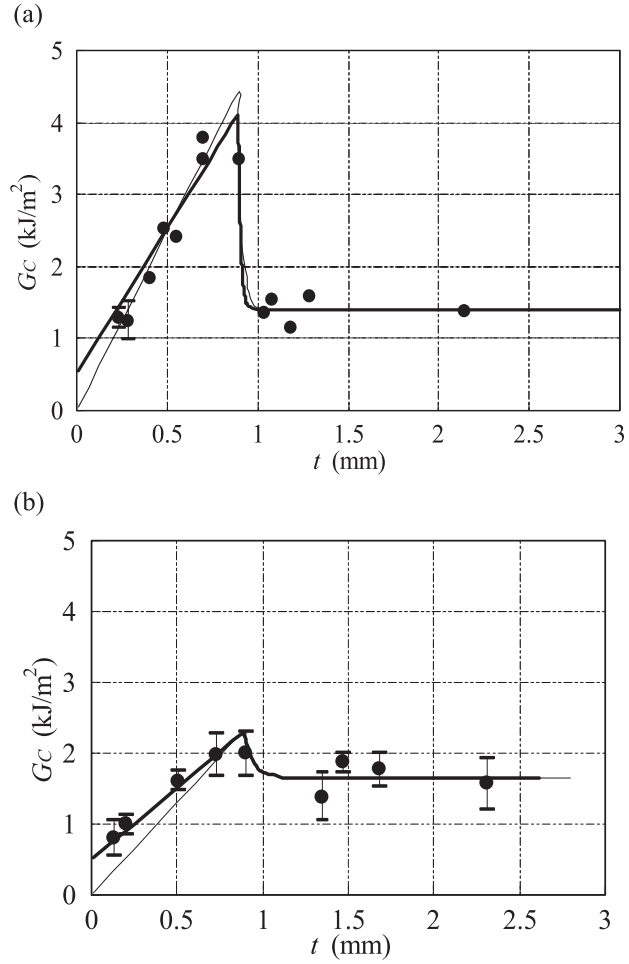

Fig. 6. Adhesive thickness effect on critical strain energy release rate of a rubber-modified epoxy adhesive bonded between two mild steel substrates. The plastic zone or FPZ height = adhesive thickness before the peak value is reached. Specimen thicknesses are (a) 50 mm and (b) 3 mm [25].

$G_{max} = 2.3$ kJ/m^2 and $G_{bulk} = 1.65$ kJ/m^2. The major difference between the results in Fig. 6a and b is the specimen thickness, $B = 50$ and 3 mm. One can be classified as plane strain and, the other, plane stress. The difference in the results also shows the boundary influence from the two free specimen boundaries in the thickness direction.

7. Discussion

The significance and usefulness of the RILEM G_F is not questioned, and its simplicity is a blessing because concrete fracture can be modelled by a fictitious crack. The current paper merely points out that all simplified models have their limitations, and a good understanding of those limitations helps us to make the right judgement on any potential problems encountered in their applications.

Although the influence of FPZ height h_{FPZ} is emphasised in the paper and used to explain the ligament or size effect on the RILEM G_F, it is not used in actual modelling. Instead, the simplicity of RILEM G_F, or of a linear constant fracture energy distribution over the entire crack area, is retained by the introduction of the bilinear local fracture energy g_f distribution. A key objective of the local g_f is to widen the global G_F application to arenas of boundary regions, where severe ligament effect exists. Most noticeably, the concept of local specific fracture energy g_f allows the determination of the size-independent RILEM G_F from small concrete specimens through Eq. (6), which, otherwise, can only be determined from very large concrete specimens, where the boundary influence can be neglected.

Clearly, the local g_f does not depreciate the usefulness of the global G_F. Using the concept of local fracture energy distribution, the RILEM G_F can be taken as a linear constant distribution or a special case of the bilinear g_f distribution, in cases where the boundary influence is small and negligible. The first constant linear g_f function in the inner zone of a concrete specimen is identical with the linear constant RILEM G_F if the boundary effect is small. The second linearly decreasing g_f function is used to model the boundary influence due to the reduction in h_{FPZ}. Recognition of the RILEM G_F as a constant fracture energy distribution is an important step towards solving its ligament effect problem, as pointed out by the local fracture energy g_f concept.

It is easy to accept that the specific fracture energy is constant in the middle of a relatively large concrete specimen, but it may be hard to conceive why the specific fracture energy reduces linearly in the boundary region. Of course, a linear g_f function in the boundary region is a simplified assumption, but is a step further in comparison with a constant RILEM G_F assumption. The EWF model deals exclusively with the same boundary influence on fracture of ductile polymer and metal specimens. The linear function shown in Eq. (7) provides an explicit support to the bilinear g_f distribution assumed for concrete. The linear g_f distribution in the boundary region of a concrete specimen, similar with that in polymer and metal, can also be proven experimentally. Eq. (4) allows the direct determination of the local g_f from experiments without using the bilinear assumption. However, the g_f distribution thus obtained also appears to be linear in the boundary region, as shown in Fig. 3c.

Probably, the thickness effect on fracture of thin adhesives [26,27] provides the most direct and convincing evidence on the influence of a plastic zone or FPZ height h_{FPZ} on fracture properties. The adhesive thickness t is identical with h_{FPZ} before t reaches the maximum thickness t_{max}. The linear relationship between h_{FPZ} and the critical strain energy release rate G_C also provides the verification on the h_{FPZ} influence in the boundary region and the resultant linearly decreasing g_f distribution.

After all the above discussions on h_{FPZ} and g_f, one would appreciate more the simplicity of RILEM G_F, as specified in Eq. (1), and its usefulness and correctness in the modelling of concrete fracture through a fictitious crack, as shown in Eq. (2). The fact that the fictitious crack model [12,13], together

with the RILEM G_F, has been embraced by so many speaks for itself. The ligament or size effect on the RILEM G_F, as pointed out in this paper, is due to the boundary influence because both h_{FPZ} and g_f decrease linearly in the boundary region. With the introduction of the local fracture energy g_f, applications of the fictitious crack model are not limited by the constant G_F assumption. The same fictitious crack can still be used to simulate concrete fracture if a cohesive stress and strain (w/w_c) relation is adopted [1,2,8].

The boundary effect on the elastic and plastic fracture of metals has commonly been discussed, even in textbooks (e.g., Ref. [28]). It explains why the LEFM is no longer applicable if a crack-tip plastic or FPZ is too close to a boundary. The elastic and plastic approach for metal and polymer has been adopted to deal with the common-size effect on concrete fracture through the influence of specimen front boundary [8,29–32]. Our most recent research shows that the overall influence from both the front and back boundaries can be combined together for finite-size specimens [33].

8. Conclusion

The common mechanism controlling the size effect on concrete fracture, the ligament effect on large scale yielding of metals and polymers, and thickness effect on adhesive joint fracture has been identified as the boundary influence in this paper. The boundary-effect model for concrete fracture, as shown in Eq. (6b), the EWF model for yielding of bulk polymer and metal, as shown in Eq. (7), and the adhesive joint thickness effect model as shown in Eq. (8a) are identical. These models, together with various experimental observations in these different material systems, show that a bilinear local fracture energy g_f distribution is adequate enough to consider the boundary influence.

The bilinear local g_f distribution allows the determination of the size-independent G_F from the size-dependent global G_f obtained from small concrete specimens, as given in Eq. (6). Testing of very large and expansive concrete specimens that are difficult to handle in most laboratories is no longer required.

Finally, the relationship between global G_f and local g_f, specified in Eq. (4), provides a simple and direct method for the determination of the g_f distribution from the RILEM G_F measurements. The importance of Eq. (4) can also be proven from the correlations shown in Eqs. (5) and (6), which provide a useful tool for determination of the size independent specific fracture energy G_F from small concrete specimens.

Acknowledgements

The financial support from the Australian Research Council under the scheme of Discovery Grant is acknowledged.

References

[1] X.Z. Hu, Fracture Process Zone and Strain Softening in Cementitious Materials, Aedificatio, Freburg, Germany, 1995 (Building Materials Series, Report No. 1, ETH, Switzerland, 1990).
[2] X.Z. Hu, F.H. Wittmann, Fracture energy and fracture process zone, Mat. Struct. 25 (1992) 319–326.
[3] RILEM TC-50 FMC, Determination of the fracture energy of mortar and concrete by means of three-point bend tests on notched beams, Mat. Struct. 18 (1985) 285–290.
[4] K. Duan, X.Z. Hu, F.H. Wittmann, Boundary effect on concrete fracture induced by non-constant fracture energy distribution, in: R. de ars, J. Mazars, G. Pijaudier-Cabot, J.G.M. van Mier (Eds.), Fracture Mechanics of Concrete Structures (Proc. FraMCoS-4), vol. 1, A.A. Balkema, Lisse, The Netherlands, 2001, pp. 49–55.
[5] K. Duan, X.Z. Hu, F.H. Wittmann, Explanation of size effect in concrete fracture using non-uniform energy distribution, Mat. Struct. 35 (2002) 326–331.
[6] K. Duan, X.Z. Hu, F.H. Wittmann, Thickness effect on fracture energy of cementitious materials, Cem. Concr. Res. 33 (4) (2003) 499–507.
[7] K. Duan, X.Z. Hu, F.H. Wittmann, Size effect on fracture resistance and fracture energy of concrete, Mat. Struct. 36 (2003) 74–80.
[8] X.Z. Hu, K. Duan, Size effect and crack bridging in coarse-microstructure composites, in: A.V. Dyskin, X.Z. Hu, E. Sahouryeh (Eds.), Structural Integrity and Fracture (The Proc. Int. Conf. on Struct. Integrity Fract. SIF 2002), A.A. Balkema, Lisse, The Netherlands, 2002, pp. 43–48.
[9] H.M. Abdalla, B.L. Karihaloo, Determination of size-independent specific fracture energy of concrete from three-point bend and wedge splitting tests, Mag. Concr. Res. 55 (2003) 133–141.
[10] B.L. Karihaloo, Fracture Mechanics and Structural Concrete, Addison Wesley Longman, London, 1995.
[11] F.H. Wittmann, X.Z. Hu, Fracture process zone in cementitious materials, Int. J. Fract. 51 (1991) 3–18.
[12] A. Hillerborg, Analysis of one single crack, in: F.H. Wittmann (Ed.), Fracture Mechanics of Concrete, Elsevier, Amsterdam, 1983, pp. 223–249.
[13] A. Hillerborg, M. Modeer, P.E. Petersson, Analysis of crack formation and crack growth in concrete by means of fracture mechanics and finite elements, Cem. Concr. Res. 6 (1976) 773–782.
[14] R.M.L. Foote, Y.W. Mai, B. Cotterell, Crack growth resistance curves in strain-softening materials, J. Mech. Phys. Solids 34 (1986) 593–607.
[15] Y.W. Mai, B. Lawn, Crack-interface bridging as a fracture resistance mechanism in ceramics: II. Theoretical fracture mechanics model, J. Am. Ceram. Soc. 70 (1987) 289–294.
[16] X.Z. Hu, Y.W. Mai, A general method for determination of crack-interface bridging stresses, J. Mater. Sci. 27 (1992) 3502–3510.
[17] F.H. Wittmann, P.E. Roelfstra, H. Mihashi, Y.Y. Huang, X. Zhang, N. Nomura, Influence of age of loading, water/cement ratio, and rate of loading on fracture energy of concrete, Mat. Struct. 20 (1987) 103–110.
[18] B. Cotterell, P. Paramasivam, K.Y. Lam, Modelling the fracture of cementitious materials, Mat. Struct. 25 (1992) 14–20.
[19] Z.P. Bazant, F.B. Lin, Nonlocal smeared cracking model for concrete fracture, J. Struct. Div. ASCE 114 (1988) 2493–2510.
[20] J. Bolander Jr., H. Hikosaka, Simulation of fracture in cement-based composites, Cem. Concr. Compos. 17 (1995) 135–145.
[21] B. Cotterell, J.K. Reddell, The essential work of plane stress ductile fracture, Int. J. Fract. 13 (1977) 267–277.
[22] Y.W. Mai, B. Cotterell, Effects of pre-strain on plane stress ductile fracture in α-brass, J. Mater. Sci. 15 (1980) 2296–2306.
[23] A.G. Atkins, Y.W. Mai, Elastic and Plastic Fracture: Metals, Polymers, Ceramics, Composites, Biological Materials, Ellis Horwood, England, 1985.
[24] P. Luna, C. Bernal, A. Cisilino, P. Frontini, B. Cotterell, Y.W. Mai,

The application of the essential work of fracture methodology to the plane strain fracture of ABS 3-point bend specimens, Polymer 44 (2003) 1145–1150.
[25] K. Duan, X.Z. Hu, Y.W. Mai, Substrate constraint and adhesive thickness effects on fracture toughness of adhesive joints, J. Adhes. Sci. Technol. 18 (2004) 39–54.
[26] A.J. Kinloch, S.J. Shaw, The fracture resistance of a toughened epoxy adhesive bonds, J. Adhes. 12 (1981) 59–77.
[27] J.H. Crews Jr., K.N. Shivakumar, I.S. Raju, Factors influencing elastic stresses in double cantilever beam specimens, in: W.S. Johnson (Ed.), Adhesively Bonded Joints: Analysis and Design, ASTM STP 981, American Society for Testing and Materials, Philadelphia, 1988, pp. 119–132.
[28] N.E. Dowling, Mechanical Behaviour of Materials, Prentice-Hall, New Jersey, 1999.
[29] X.Z. Hu, Size effect in toughness induced by crack close to free edge, in: H. Mihashi, K. Rokugo (Eds.), Fracture Mechanics of Concrete Structures (Proc. of FRAMCOS-3), Aedificatio, Freiburg, 1998, pp. 2011–2020.
[30] X.Z. Hu, F.H. Wittmann, Size effect on toughness induced by crack close to free surface, Eng. Fract. Mech. 65 (2000) 209–221.
[31] X.Z. Hu, An asymptotic approach to size effect on fracture toughness and fracture energy of composites, Eng. Fract. Mech. 69 (2002) 555–564.
[32] K. Duan, X.Z. Hu, Asymptotic analysis of boundary effects on fracture properties of notched bending specimens of concrete, in: A.V. Dyskin, X.Z. Hu, E. Sahouryeh (Eds.), Structural Integrity and Fracture (The Proc. Int. Conf. on Struct. Integrity Fract. SIF 2002), A.A. Balkema, Lisse, The Netherlands, 2002, pp. 19–24.
[33] K. Duan, X.Z. Hu, F.H. Wittmann, Asymptotic analysis of boundary effects on fracture properties of quasi-brittle materials, Proc. Int. Symp. on Macro-, Meso-, Micro- & Nano- Mechanics of Materials (MM2003), Hong Kong, pp. 103–105.